

NOVELLA: Nonvolatile Last-Level Cache Bypass for Optimizing Off-Chip Memory Energy

Aritra Bagchi¹, Ohm Rishabh², and Preeti Ranjan Panda¹

I. INTRODUCTION

Abstract—Contemporary multiprocessor systems-on-chips (MPSoCs) continue to confront energy-related challenges, primarily originating from off-chip data movements. Nonvolatile memories (NVMs) emerge as a promising solution with their high-storage density and low leakage, yet they suffer from slow and expensive write operations. Writebacks from higher-level caches and responses from off-chip memory create significant contention at the shared nonvolatile last-level cache (LLC), affecting system performance with increased queuing for critical reads. Previous research primarily addresses the performance issues by trying to mitigate contention through the bypassing of NVM writes. Nevertheless, off-chip memory energy, one of the most critical components of system energy, remains unaddressed by state-of-the-art bypass policies. While certain energy components, such as leakage and refresh, depend on system performance, performance-optimizing bypass policies may not ensure energy efficiency. Aggressive bypass decisions aimed only at performance enhancement could degrade cache reuse, potentially outweighing reductions in leakage and refresh energies with the increase in off-chip dynamic energy. While both performance and off-chip memory energy are influenced by both cache contention and reuse, the tradeoffs for achieving optimal performance versus optimal energy are different. We introduce nonvolatile last-level cache bypass for optimizing off-chip memory energy (NOVELLA), a novel bypass policy for the nonvolatile LLC, to optimize off-chip memory energy by exploiting tradeoffs between cache contention and reuse, achieving a balance across different components of the energy. Compared to a naïve no-bypass baseline, while state-of-the-art reuse-aware bypass solutions reduce off-chip memory energy consumption by up to 8%, and a contention- and reuse-aware bypass baseline by 12%, NOVELLA achieves significant energy savings of 21% across diverse SPEC workloads.

Index Terms—Cache bypass, energy-efficient memory systems, last-level cache (LLC), memory, nonvolatile memory (NVM).

Manuscript received 11 August 2024; accepted 12 August 2024. This article was presented at the International Conference on Compilers, Architectures, and Synthesis for Embedded Systems (CASES) 2024 and appeared as part of the ESWEEK-TCAD Special Issue. This article was recommended by Associate Editor S. Dailey. (Corresponding author: Aritra Bagchi.)

Aritra Bagchi is with the Department of Computer Science and Engineering, Indian Institute of Technology Delhi, New Delhi 110016, India (e-mail: aritra.bagchi@cse.iitd.ac.in).

Ohm Rishabh is with the Department of Electrical Engineering, Indian Institute of Technology Delhi, New Delhi 110016, India (e-mail: ohm.v@alumni.iitd.ac.in).

Preeti Ranjan Panda is with the Department of Computer Science and Engineering and the Khosla School of IT, Indian Institute of Technology Delhi, New Delhi 110016, India (e-mail: panda@cse.iitd.ac.in).

Digital Object Identifier 10.1109/TCAD.2024.3446720

SYSTEM-LEVEL energy efficiency is a pivotal aspect of modern SoC design. Although contemporary multiprocessor systems-on-chips (MPSoCs) integrate several processor cores and accelerators, off-chip data movements remain the energy Achilles heel, responsible for over 60% of the total system energy [1]. Last-level cache (LLC) serves as the final line of defense against expensive off-chip accesses, making the requirement for larger LLCs crucial in today's systems. As conventional technologies, such as SRAM and DRAM, consume excessive leakage power when scaled, nonvolatile memory (NVM) technologies, such as STT-MRAM, PCM, DWM, ReRAM, and FeRAM, have received serious research attention because of their higher-storage densities and low-leakage power. However, NVMs suffer from major limitations. STT-MRAM, which offers the highest endurance among all other NVMs and emerges as one of the most promising alternatives to SRAM in designing future LLCs, still struggles with inefficient write operations, which are 2-5× slower than reads [2], [3].

Fig. 1 illustrates the architectural overview of our MPSoC. The first two levels of caches (L1, L2) are private to each processor core, whereas the LLC is shared among all cores. As fast access speed is a crucial requirement for private caches, they are typically implemented with SRAM. To meet emerging applications' demand for reducing costly off-chip memory accesses through larger LLCs, we target an NVM implementation for the LLC, which offers more density at low leakage. When a core requests data, it first checks its private caches. If the data is not found (cache miss), a *read* request (Arrow ①) is sent to the LLC, where it is enqueued into the *request queue*. If the data is present in the LLC (cache hit), it responds to the corresponding L2 cache with the requested data. Otherwise, the request is sent to the off-chip main memory. Upon fetching the data from the main memory, a response arrives back at the LLC. The LLC controller then creates a copy of the response data and forwards it to the requesting core for maintaining its progress (Arrow ③). The original response is inserted into the *response queue* for later writing (Arrow ④). Apart from responses, evictions from L2 caches generate another source of NVM write operations, known as *writebacks*, which are enqueued into the request queue (Arrow ②). Because NVM writes are 2 – 5× slower than reads (shown in different colors, Fig. 1), writebacks and responses contend with read requests for the available LLC bandwidth, introducing longer queuing delays

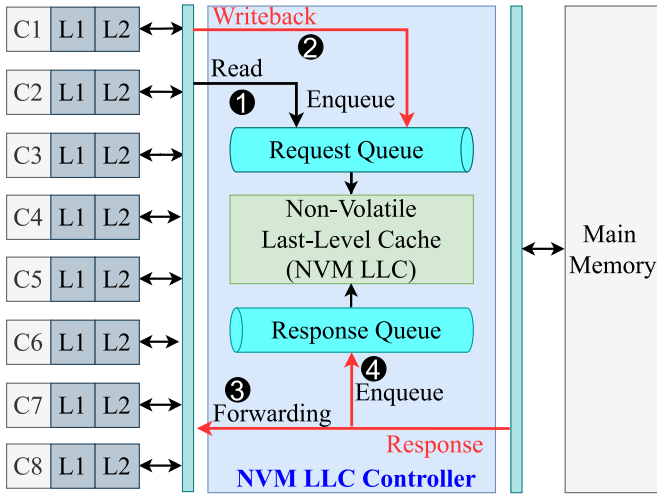


Fig. 1. Overview of system architecture. Writebacks from higher-level caches and responses from off-chip main memory exacerbate LLC contention, delaying critical reads, and affecting overall system performance.

- 2) A balance across different memory energy components is manifested by tradeoffs between the implications of bypass decisions on NVM cache reuse and contention. We investigate these tradeoffs and exploit them in NOVELLA.
- 3) Energy implications of bypassing different sources of NVM writes vary across different workloads. We identify and leverage such application-specific tradeoffs in NOVELLA.
- 4) To model the asymmetric implications of NVM reads and writes on shared LLC contention, we enhanced the cache timing model of the gem5 simulator and plan to make an open-source release of the enhancement.

The remainder of this article is organized as follows. Section II summarizes relevant prior works, Section III motivates the key energy tradeoff, Section IV discusses the proposed policy, and Section V presents its hardware implementation. Section VI covers the experimental setup, evaluation, results, and overheads, followed by the conclusion in Section VII.

II. RELATED WORK

Prior works addressed NVM cache performance and energy challenges primarily through hardware-based approaches [3], [8], [12], [13], emphasizing cache bypass techniques to address inefficient NVM writes. Korgaonkar et al. [3] proposed write congestion aware bypass (WCAB), which, based on the average occupancy of the request queue and the liveness of data, bypasses writebacks to mitigate NVM cache contention. WCAB primarily focused on enhancing system performance but also estimated its impact on memory energy, serving as one of our baselines in Section VI. Using sampling predictors, Ahn et al. [7] bypassed various sources of redundant NVM writes to reduce NVM cache energy. Zhang et al. [9] designed an NVM cache bypass technique based on a theoretical model of data reuse statistics. Analytically estimating the benefits of caching data in terms of their impact on access latency, Wang et al. [8] proposed a runtime bypass policy for NVM writes. A selective NVM cache inclusion policy is designed by Cheng et al. [14] to store only a subset of data from higher-level caches for improving NVM cache energy.

Bypass policies have also been explored for conventional caches. Wu et al. [10] proposed a signature-based hit predictor (SHiP), which associates each cache reference with a signature, incrementing a counter on hits and decrementing on evictions without reuse. SHiP bypasses a cache fill if its signature corresponds to a counter of value zero, anticipating distant reuse. Li et al. [11] proposed a bypass policy that tracks reuse distances of cache fills and associated victims, caching data only when the fill has incurred reuse distance less than that of associated victims in the past. Park et al. [15] proposed a bypass first policy (BFP), bypassing fills by default, and caching them later if they are predicted to offer spatial or temporal reuse. Bagchi et al. [6] proposed a response bypass mechanism that dynamically exploits the tradeoff between cache contention and reuse to enhance system throughput, addressing contention concerns overlooked by other policies. These policies are considered baselines in Section VI.

for critical reads, thereby creating performance bottlenecks. Such contention is a major concern even in contemporary MPSoCs with SRAM LLCs [4], [5], [6], and gets aggravated in next-generation MPSoCs with NVM LLCs.

Prior works unanimously focused on improving system performance or reducing NVM cache energy [3], [7], [8], [9], neglecting off-chip memory energy considerations. However, across our real-world workloads, off-chip memory accounts for 64% of the total memory-system energy, with LLC contributing only around 9%. The off-chip memory energy comprises three components: 1) *static*; 2) *dynamic*; and 3) *refresh*. Static and refresh energies, accounting for 60% of the total off-chip memory energy, correlate closely with overall system performance, while the dynamic component is influenced by LLC reuse, which controls the volume of off-chip memory traffic. Prior bypass policies either overemphasize cache reuse [3], [7], [10], [11], or mitigate contention for enhancing system performance at the expense of cache reuse [6]. An excessively aggressive bypass, despite having the potential for enhancing performance, could affect cache reuse and overpower improvements in static and refresh energies with the increase in dynamic memory energy (DynE). Both performance and off-chip memory energy are influenced by cache contention and reuse, but the tradeoffs for optimizing performance versus energy differ. We exploit this tradeoff in NOVELLA, a dynamic cache bypass policy for NVM writes, to mitigate off-chip memory energy bottlenecks and help scale next-generation systems against the memory power wall. In an NVM cache, any write operation creates bottlenecks, so NOVELLA is designed to make bypass decisions for all sources of NVM writes. Our major contributions are summarized as follows.

- 1) While existing bypass policies for NVM cache focus only on performance and/or cache energy, we, to the best of our knowledge, are the first to primarily target optimizing off-chip memory energy through NVM cache bypass.

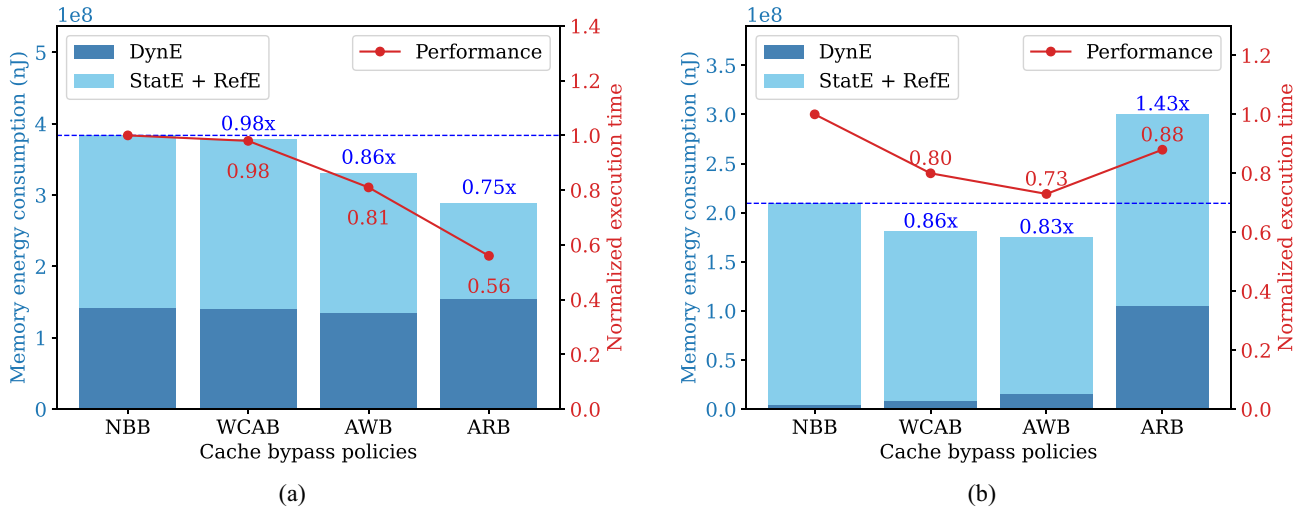


Fig. 2. Motivational example demonstrating off-chip memory energy and performance profiles of two SPEC workloads (from Table III). In (a), performance enhancements lead to overall energy efficiency when LLC reuse (which controls dynamic energy) is minimally impacted. In (b), bypassing NVM writes of certain types degrades LLC reuse significantly, increasing DynE so much that it outweighs reductions in static and refresh energies achieved through performance enhancement. This motivates the need for balancing different off-chip memory energy components to achieve overall energy efficiency.

In hybrid SRAM-NVM caches, write-intensive data are dynamically identified and migrated to SRAM for mitigating NVM write overheads [13], [16]. NVM caches are also implemented with regions of different retention times, while placing data according to the cache access pattern [12], [17], [18]. Zhou et al. [19] proposed a circuit-level optimization to proactively terminate redundant NVM writes. Zero-valued NVM cache data are encoded by Jung et al. [20] to save NVM write energy. To circumvent DRAM scaling issues, high-density NVMs (e.g., PCM) have been explored for main memories [21]. Researchers also explored energy-aware memory controller policies. Wu et al. [22] dynamically migrated memory pages to consolidate shorter idle periods into longer ones, therefore exploiting the low-power states to control the background power consumption. Lai et al. [23] demoted ranks with less critical reads to low-power modes, while prioritizing the service of critical reads for maintaining performance. Energy-aware memory controller policies [22], [23] are orthogonal to our cache bypass-based approach and could be applied in parallel for further energy efficiency.

III. MOTIVATION

For next-generation NVM caches, bypass techniques are shown to be beneficial for improving overall system performance as well as reducing cache energy consumption [3], [7], [8], [9], both of which are synergistic objectives for cache bypass policies. These bypass policies circumvent the performance penalties of slow NVM writes, reducing the cache leakage energy, while also reducing the cache dynamic energy as a direct consequence of bypassing some NVM writes. Nevertheless, prior works did not explore the potential of NVM cache bypass in addressing off-chip memory energy, which is the most challenging system energy bottleneck.

For an LLC, which is shared by an increasing number of cores and accelerators, both contention and reuse are

crucial system-level factors controlling the consumption of off-chip memory energy. Bypassing NVM writes aggressively could alleviate LLC contention and reduce the consumption of static and refresh components of off-chip memory energy through improvements in overall system performance. However, aggressive bypass could disturb LLC reuse (or locality) and, if not controlled carefully, could outweigh the energy efficiency achieved through performance improvements. Also, while the latencies for multiple off-chip memory accesses can be hidden (*memory-level parallelism*), the energy overheads cannot be hidden in the same manner as delays. Therefore, an energy-efficient bypass policy for NVM LLC should carefully consider this key tradeoff. Based on profiling of real-world SPEC applications (from the pool of evaluation workloads in Table III, Section VI-A) with a state-of-the-art NVM cache bypass solution [3] and a few baseline strategies, we demonstrate the tradeoff in detail as follows.

Fig. 2 illustrates the trends in different components of off-chip memory energy alongside corresponding trends in system performance measured as the workload execution time. Fig. 2a and b show energy and performance profiles of two SPEC workloads, i.e., mixes 10 and 2, respectively, from Table III, Section VI-A. Energy components are plotted along the left Y-axis (in nanojoules), while the normalized execution time is shown along the right Y-axis. In Fig. 2, the DynE, influenced by overall LLC reuse, is depicted separately in each bar plot, while the static and refresh energies, both dependent on overall execution time, are combined (StatE + RefE). For each mix, results across four different cache bypass policies are presented along the X-axis. While WCAB [3] is the state-of-the-art NVM cache bypass policy, the other three are constructed by us. The aggressive writeback bypass (AWB) bypasses writebacks aggressively, writing all responses. Conversely, aggressive response bypass (ARB) bypasses responses, caching all writebacks. The no-bypass baseline (NBB) is a naïve policy serving as a global baseline. NBB does not apply any bypass, writing all data to

247 NVM cache. The execution time of each policy is normalized
248 relative to that of NBB.

249 In Fig. 2(a), we observe that the dynamic off-chip memory
250 energy remains almost the same in NBB and WCAB, whereas
251 AWB and ARB lead to a 4% reduction and a 9% increment
252 in the dynamic off-chip memory energy compared to NBB.
253 As the implications of these bypass strategies on LLC locality
254 are similar, the dynamic energy does not undergo drastic
255 variations. WCAB, AWB, and ARB mitigate NVM LLC
256 contention to varying extents, resulting in 2%, 19%, and 44%
257 improvements in overall execution time, respectively, over
258 NBB. As a result, the static and refresh energies are also
259 reduced almost proportionally, leading to overall improve-
260 ments in off-chip memory energy consumption by 2%, 14%,
261 and 25% over NBB for WCAB, AWB, and ARB, respectively.
262 In summary, Fig. 2(a) demonstrates a real-world execution
263 scenario where improvements in overall system performance
264 lead to reductions in off-chip memory energy, given the similar
265 impacts of bypass decisions on LLC locality.

266 Fig. 2(b) presents another scenario where different bypass
267 policies have considerably different implications for LLC
268 locality. For instance, WCAB enhances performance by 20%
269 over NBB, resulting in a 14% reduction in overall off-chip
270 memory energy consumption compared to NBB. Similarly, for
271 AWB, a 27% reduction in the overall execution time leads
272 to a 17% reduction in the consumption of off-chip memory
273 energy. For WCAB and AWB, despite the dynamic component
274 of off-chip memory energy increasing over NBB by $1.71\times$ and
275 $3.25\times$, respectively, the improvements in system performance
276 successfully translate to overall energy reductions. However,
277 the situation differs significantly for ARB, which, in its attempt
278 to mitigate LLC contention through ARB, disrupts cache
279 locality to such an extent that the dynamic off-chip memory
280 energy escalates by a factor of $21.68\times$ over NBB. This drastic
281 deterioration in dynamic energy outweighs the comparatively
282 smaller reductions in the other two performance-dependent
283 energy components (static and refresh), leading to a 43%
284 increase in overall off-chip memory energy. Fig. 2(a) and (b)
285 emphasize the tradeoffs between different components of off-
286 chip memory energy, with one being dependent on LLC
287 reuse and the other two being correlated to overall system
288 performance. Also, bypassing different sources of NVM writes
289 (writebacks versus responses) explores this tradeoff dispropor-
290 tionately for different workloads. This important observation
291 motivates us to develop an adaptive bypass policy for NVM
292 LLC that strategically exploits this tradeoff and dynamically
293 modulates its emphasis on mitigating LLC contention and
294 maintaining LLC reuse so as to reduce the consumption of
295 off-chip memory energy across diverse workloads.

296 IV. PROPOSED METHODOLOGY

297 We introduce nonvolatile LLC bypass for optimizing
298 off-chip memory energy (NOVELLA), which dynamically
299 bypasses NVM writes to reduce off-chip memory energy
300 consumption. NVM writes are significantly slower than reads,
301 exacerbating LLC contention. Bypassing NVM writes could
302 enhance performance by alleviating LLC contention. However,

our focus is on reducing off-chip memory energy. By exploit- 303
ing tradeoffs between LLC contention and reuse for balancing 304
different memory energy components, NOVELLA achieves 305
overall energy efficiency. 306

307 A. Key Ideas and Execution Scenarios

308 We present an overview of NOVELLA by illustrating differ- 308
ent execution scenarios and how NOVELLA adapts its bypass 309
decision for different sources of NVM writes across these 310
scenarios. For this purpose, we consider three categories of 311
real-world applications: 1) LLC agnostic (LA); 2) LLC heavy 312
(LH); and 3) memory heavy (MH). While LA applications 313
produce less LLC contention, the other two result in significant 314
contention. However, while LH applications lead to most of 315
their memory accesses being served from LLC (high-LLC 316
access rate with the majority producing hits), MH applications 317
lead to most of their accesses being served from off-chip main 318
memory (high-LLC access rate with the majority producing 319
misses). The key ideas are summarized as follows. 320

- 321 1) When MH applications are co-executed, there is already 321
significant pressure on off-chip memory due to the 322
majority of memory accesses being directed there, caus- 323
ing us to be conservative in bypassing both sources of 324
NVM writes. Although an aggressive bypass could miti- 325
gate LLC contention, it could worsen DynE significantly, 326
leading to overall energy inefficiency. 327
- 328 2) The two sources of NVM writes, writebacks and 328
responses, have asymmetric implications for off-chip 329
memory energy. While bypassing responses may 330
increase memory energy by compromising LLC locality 331
and potentially losing future LLC hits, bypassed write- 332
backs not only risk converting future LLC hits into 333
misses but also immediately increase off-chip memory 334
traffic, affecting off-chip memory energy in a more 335
direct way. 336
- 337 3) Responses exhibit a range of reuse patterns, with some 337
being more valuable than others. Certain responses may 338
be deemed *dead* if they are never referenced between 339
their fill and eviction. We prefer caching of more 340
important response data while potentially bypassing the 341
rest. Such selective response writes could help mitigate 342
LLC contention, but without increasing off-chip memory 343
traffic significantly. If the underlying reuse profile is 344
more diverse, selective writes could also enhance cache 345
locality by preventing premature evictions of useful data. 346
- 347 4) For the co-execution of LA applications, where the 347
majority of memory accesses are handled by private 348
caches, a significant portion of responses filled to LLC 349
are not reused from LLC. However, evicted cache lines 350
from private caches (writebacks) stored in LLC present 351
more opportunities for reuse. Therefore, despite the main 352
memory experiencing less pressure, we prefer caching 353
writebacks while selectively caching useful responses. 354

355 In Fig. 3, we present four execution scenarios: cases A (co- 355
execution of LH applications) and B (co-execution of MH 356
applications), C (co-execution of LH and MH applications), 357
and D (co-execution of LA applications) in Fig. 3(a)–(d), 358

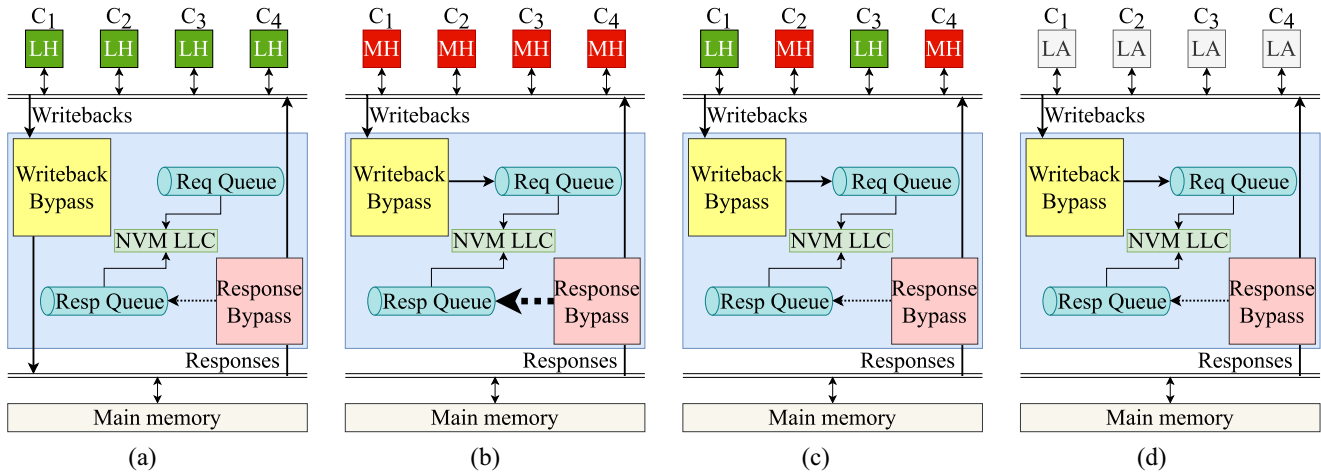


Fig. 3. Illustrative example of NOVELLA, demonstrating NVM write bypass decisions across different execution scenarios. (a) *Case A*: As main memory experiences less pressure, we opt for writeback bypass because of their high contention and low-reuse potential, while selectively caching responses based on their predicted usefulness. (b) *Case B*: We opt for caching of writebacks and conservative bypassing of responses due to the main memory already experiencing significantly high pressure, generated by high volume of off-chip memory traffic. (c) *Case C*: We opt for caching of writebacks because of the off-chip main memory experiencing considerable pressure, while selectively caching responses based on their predicted usefulness. (d) *Case D*: Despite the main memory experiencing low pressure, we prefer caching writebacks because of their higher-reuse potential, while selectively caching responses based on their predicted usefulness.

359 respectively. For a simpler representation, we do not show
 360 private caches and cores separately but highlight LLC con-
 361 trollers, which comprise two different modules for making
 362 bypass decisions for two different sources of NVM writes:
 363 1) *Writeback Bypass* and 2) *Response Bypass*. These modules
 364 control the flow of incoming NVM writes into their respective
 365 controller queues (*Req Queue* and *Resp Queue*), enqueueing
 366 a writeback or a response only if its data is decided to be
 367 cached. For illustrative purposes, we show a four-core system.
 368 In Fig. 3, conditional actions (e.g., enqueueing of responses) are
 369 represented by *dotted* arrows, whereas actions that are always
 370 performed (e.g., response forwarding, scheduling of pending
 371 accesses from the queues into the NVM LLC, enqueueing of
 372 writebacks) are shown in *solid* arrows. While the thick dotted
 373 arrow indicates frequent actions, thin dotted arrows represent
 374 relatively infrequent ones. Building upon the ideas discussed
 375 above, we outline NOVELLA’s bypass decisions as follows.

376 1) *Case A*: In this case [Fig. 3(a)], responses are found
 377 to be more crucial than writebacks from the perspective of
 378 LLC data reuse. Writebacks, on the other hand, do not impact
 379 LLC locality as strongly as responses do, but contribute more
 380 toward LLC contention. As previously discussed (Point 1),
 381 the main memory experiences relatively less pressure in
 382 case A because of LLC filtering the majority of memory
 383 accesses from reaching main memory. Therefore, we can
 384 afford to bypass writebacks (solid arrow in Fig. 3(a) directing
 385 writebacks toward the main memory) to alleviate the NVM
 386 LLC contention. We take response reuse into considera-
 387 tion while making bypass decisions for them (Point 3). As
 388 highlighted in Point 1, we have the liberty to be select-
 389 ive in caching responses in case A [indicated by a thin
 390 dotted arrow leading responses to the response queue in
 391 Fig. 3(a)].

392 2) *Case B*: In this case [Fig. 3(b)], we experimentally
 393 observe that even an aggressive form of writeback bypass
 394 (such as AWB, discussed in Section III) could enhance

395 system performance minimally, but ends up increasing off-
 396 chip memory energy considerably. Therefore, because of the
 397 critical impact of bypassing writebacks on memory energy
 398 (Point 2), particularly in this scenario (Point 1), we prefer to
 399 cache writebacks, as represented by the solid arrow following
 400 writebacks into the LLC request queue in Fig. 3(b). On
 401 the other hand, bypassing responses very aggressively helps
 402 mitigate NVM LLC contention (and improve performance)
 403 but at the expense of degraded LLC reuse, which might
 404 outweigh the improvements in static and refresh energies
 405 with increased DynE. Therefore, we are conservative also
 406 in bypassing responses (Point 1), as indicated by the thick
 407 dotted arrow in Fig. 3(b) leading responses to the response
 408 queue. We prioritize caching writebacks, following the most
 409 conservative approach, due to their asymmetrically stronger
 410 impact on memory dynamic energy compared to the other
 411 NVM write source (as indicated in Point 2).

412 3) *Case C*: In this diverse execution scenario [Fig. 3(c)],
 413 we prefer caching writebacks [as shown by the solid arrow
 414 leading writebacks to the LLC request queue in Fig. 3(c)]
 415 because of their crucial impact on the energy of off-chip main
 416 memory (Point 2), which already experiences considerable
 417 memory traffic from MH applications (Point 1). As indicated
 418 in Point 3, responses exhibit diverse reuse behavior in this
 419 case. This creates opportunity for us to be selective in caching
 420 only useful responses, as shown in Fig. 3(c) by the thin
 421 dotted arrow directing responses to the LLC response queue.

422 4) *Case D*: In this scenario [Fig. 3(d)], although the co-
 423 execution of LA applications exerts less pressure on off-chip
 424 main memory due to limited memory accesses beyond private
 425 L2 caches, we prioritize caching writebacks [as shown by
 426 the solid arrow leading writebacks to the request queue in
 427 Fig. 3(d)] due to their high-LLC reuse potential (Point 4).
 428 Meanwhile, responses demonstrate comparatively lower reuse
 429 at LLC compared to writebacks, allowing us to be selective
 430 in caching only useful response data.

431 B. NOVELLA Methodology

432 The NOVELLA controller has two major components:

- 433 1) *Writeback Bypass*: Each time an evicted dirty cache line
434 from one of the higher-level caches arrives at NVM
435 LLC, we make a decision regarding whether to write the
436 data into LLC or bypass it. If the data is selected to be
437 written, we insert the writeback into the request queue.
438 Otherwise, we send the writeback to the main memory
439 to store the updated data there.
- 440 2) *Response Bypass*: Whenever a response from the main
441 memory reaches NVM LLC, we immediately for-
442 ward a copy of the data to the core waiting for it.
443 Simultaneously, we make a decision regarding whether
444 to write the data into LLC. If so, we insert the response
445 into the response queue. Otherwise, the response is
446 simply dropped, as the data has already been forwarded.

447 Based on the ideas discussed in Section IV-A, we make
448 runtime bypass decisions for writebacks and responses. This
449 involves identifying cases A, B, C, and D at runtime. While a
450 lower-LLC access rate indicates case D (co-execution of LA
451 applications), higher-access rates correspond to the other three
452 scenarios, i.e., cases A, B, and C. Among these three cases, a
453 significantly low-LLC miss rate indicates case A (co-execution
454 of LH applications), a much higher-miss rate represents case
455 B (co-execution of MH applications), while intermediate miss
456 rate values correspond to case C (co-execution of both LH and
457 MH applications).

458 Algorithm 1 describes the steps involved in NOVELLA.
459 While Lines ①- ⑦ capture the steps involved in *Writeback*
460 *Bypass*, Lines ⑧- ⑳ discuss steps involved in *Response*
461 *Bypass*. When a writeback W_{Acc} reaches NVM LLC (line
462 ①), we check whether the LLC access rate (AR) is above a
463 threshold (AR_{Th}), and the miss rate (MR) is within a certain
464 lower threshold, i.e., MR_{ThL} (line ②). If so, we identify
465 the execution scenario to be case A, and decide to bypass
466 W_{Acc} (line ⑤). Because writebacks create significant LLC
467 contention in case A (discussed in Section IV-A1), such bypass
468 decisions help alleviate NVM LLC contention. However, in
469 case the data for W_{Acc} , i.e., W_{Blk} , is already present in LLC,
470 we invalidate the data to prevent any future request from
471 fetching stale data from the LLC (line ④). In all other
472 execution scenarios (cases B, C, or D), we decide to cache
473 the writeback data, and therefore, insert W_{Acc} into the LLC
474 request queue (line ⑦).

475 When a response W_{Acc} returns from the main memory con-
476 taining the requested data, we create a copy of it (W'_{Acc} , line
477 ⑨) and forward it to the higher-level cache (line ⑩). This
478 facilitates the requesting processor core to obtain data faster
479 and maintain progress. Meanwhile, we decide whether to write
480 the response or bypass it (Lines ⑪- ㉑). For this decision,
481 we estimate whether the response data is useful. In cases C
482 and D, we assess the usefulness of responses differently than
483 in the other two cases, as a single criterion is not effective
484 across all four cases (more insight in Section VI-B). Again, to
485 identify different execution scenarios, we use both LLC access
486 and miss rates. If the access rate (AR) is low, we identify the
487 scenario as case D (line ⑪) and consult the reuse prediction

Algorithm 1: NOVELLA: Nonvolatile LLC Bypass for Optimizing Off-Chip Memory Energy

Input: W_{Acc} : Write access to NVM LLC
Input: W_{Blk} : Target LLC block for NVM write
Input: MR: NVM LLC miss rate
Input: AR: NVM LLC access rate
Input: $DeadC_{Blk}$: Number of past dead fills for W_{Blk}
Input: $FillC_{Blk}$: Number of past fills for W_{Blk}
Input: RC: Predicted RC for W_{Acc}
Input: MR_{ThL} and MR_{ThH} : Lower and higher thresholds on NVM LLC miss rate
Input: AR_{Th} : Threshold on NVM LLC access rate
Input: DP_{Th} : Threshold on W_{Blk} 's dead probability
// **Writeback Bypass**
1 **if** W_{Acc} is a writeback **then**
2 **if** $MR < MR_{ThL}$ AND $AR > AR_{Th}$ **then**
3 **if** $W_{Blk} \neq \text{null}$ **then**
4 Invalidate(W_{Blk}) // upon a cache
5 hit, invalidate the data
6 Send W_{Acc} to main memory
7 **else**
8 Enqueue W_{Acc} to the request queue
9 **else**
10 // **Response Bypass**
11 $W'_{Acc} = Copy(W_{Acc})$ // creating a
12 forwardable copy of data
13 Forward W'_{Acc} to higher-level cache
14 **if** $AR \leq AR_{Th}$ **then**
15 **if** $RC > 0$ **then**
16 // data anticipated useful
17 Enqueue W_{Acc} to the response queue
18 **else**
19 **if** $MR \geq MR_{ThL}$ AND $MR < MR_{ThH}$ **then**
20 **if** $RC > 0$ **then**
21 // data anticipated useful
22 Enqueue W_{Acc} to the response queue
23 **else**
24 $DP_{Blk} = \left(\frac{DeadC_{Blk}}{FillC_{Blk}} \right)$
25 **if** $DP_{Blk} < DP_{Th}$ **then**
26 // data anticipated useful
27 Enqueue W_{Acc} to the response queue

table (RPT), a small buffer maintaining the reuse history of 488
certain prior responses [11]. Each RPT entry comprises a 3- 489
bit saturating counter. We index into the RPT using hashed 490
instruction program counter (PC) of the incoming response. 491
Initially, all the reuse counters in RPT are reset to 0. If the 492
hashed instruction PC of the incoming response W_{Acc} matches 493
against an existing entry in the RPT, the corresponding counter 494
is incremented. When RPT becomes full and there is a need 495
to allocate a new entry, we evict the oldest entry. So, when the 496

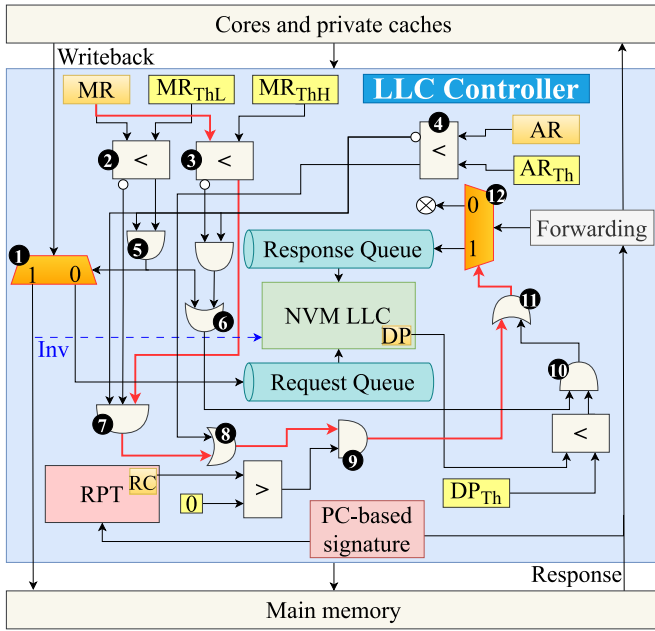


Fig. 4. Hardware implementation of NOVELLA controller. Demultiplexers ① and ⑫ execute the decisions taken for LLC writebacks and responses, respectively, regarding whether to bypass them or insert them into their respective controller queues for LLC writes. The critical path is shown in red.

access rate is low, we decide to bypass W_{Acc} if its predicted reuse (RC) is zero; otherwise, we enqueue W_{Acc} into the response queue for writing data later (line ⑬). If the access rate is high (line ⑭), and the miss rate lies in between MR_{ThL} and MR_{ThH} (line ⑮), we identify the scenario as case C and decide to write responses of nonzero reuse count (RC), as estimated from RPT (line ⑰). When the access rate is high (line ⑭), but the miss rate is below MR_{ThL} (case A) or above MR_{ThH} (case B), we assess the usefulness of the response fill by calculating the current probability of it being dead, i.e., DP_{Blk} , based on the fill history. To compute the dead-probability, we divide the number of dead fills so far for the cache block ($DeadC_{Blk}$) by the number of times the block is filled so far ($FillC_{Blk}$), as indicated in line ⑲. A block-fill is marked dead if we observe no reuse for it before its eviction. If the probability exceeds a certain threshold, DP_{Th} , we anticipate the fill to be dead and decide to bypass the response. Otherwise (line ⑳), we insert the response into the response queue for a future write (line ㉑). While AR_{Th} is decided from LLC access profiles of our workloads, the size of the RPT, miss rate thresholds (MR_{ThL} and MR_{ThH}), and dead probability threshold (DP_{Th}) are determined through sensitivity analysis.

V. CONTROLLER IMPLEMENTATION

In Fig. 4, we illustrate the implementation of NOVELLA controller. The miss and access rates of NVM LLC (MR, AR) and the other thresholds are available as registers inside the LLC controller. Using gate ⑤, we identify whether the execution scenario resembles case A, and, based on the

output of ⑤, demultiplexer ① decides whether to send the writeback to the main memory (bypass) or enqueue it into the request queue (write). To maintain functional correctness, we send a control signal from the bypass path of the demultiplexer ① to the LLC so as to invalidate the existing cache block in case of an LLC hit. In Fig. 4, this control signal, named *Inv*, is represented by a dotted blue line.

The output of AND gate ⑦ indicates case C, while the output of gate ⑥ represents cases A or B. Combining the output of gate ⑦ and the output of comparator ④ which indicates the access rate to be within AR_{Th} (i.e., case D), OR gate ⑧ represents scenarios where NOVELLA consults the RPT to estimate the reuse of an incoming response. For that, we use hashed instruction PC of the instruction corresponding to the response cache block as our signature. The bit-width of the signature determines the size of the RPT, with RPT containing 2^K entries if the signature is of K bits. In Section VI-F, we empirically determine K with a sensitivity analysis. If the predicted reuse (RC) is greater than zero, we signal the demultiplexer ⑫, through gates ⑨ and ⑪, to consider caching the response and enqueue it into the response queue. If RC is zero, we signal the demultiplexer ⑫ to drop the response (bypass). For cases A or B, indicated by the outcome of gate ⑥, we estimate the dead probability (DP) of the response fill using the cache block's fill history, recorded as additional cache metadata. We signal demultiplexer ⑫, through gates ⑩ and ⑪, to bypass the response if the dead probability is beyond the threshold DP_{Th} . If a response is decided to be bypassed, we simply drop the response (represented in Fig. 4 by the symbol \otimes), as the data for every response is forwarded to the cores.

For any incoming NVM LLC write, NOVELLA's decisions can be processed in parallel to the actual service of accesses from the controller queues. Such decisions involve combinational circuits (the critical path is highlighted in Fig. 4), and the only scenario it lies on the critical path is when there are no pending accesses in any of the controller queues and the LLC is idle. However, in our experiments across diverse SPEC workloads, we did not observe this scenario.

VI. EXPERIMENTS AND RESULTS

A. Setup

We use the gem5 simulator for experimental evaluation. Table I captures the details of our underlying system architecture. Essential cache parameters are collected from CACTI and NVSim for 22 nm technology node. To measure DRAM energy consumption, we use DRAMPower [24] tool, which extracts from gem5 performance counters necessary for the energy calculation. We use gem5's system emulation (SE) mode, which offers limited support for SPEC CPU 2017 benchmarks. Therefore, we use SPEC CPU 2006 benchmarks, known to offer memory access characteristics comparable to that of SPEC CPU 2017 benchmarks [25]. We fast-forward through 1 billion instructions, warm up caches for an additional 150 million instructions, and subsequently execute 250 million instructions for any workload. For characterizing

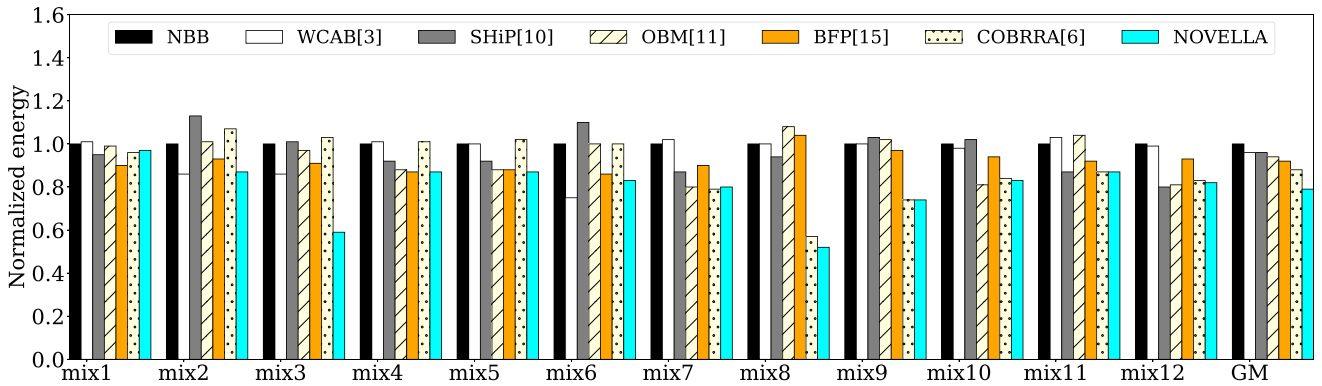


Fig. 5. Comparison of DRAM energy consumption for NOVELLA and other baselines.

TABLE I
SYSTEM CONFIGURATIONS

System Unit	Configuration
CPU	8 X86@2 GHz out-of-order CPU cores
L1 (SRAM)	Private, 32KB L1-D/I, 64B cache line, 8-way set-associative, parallel-access, tag and data latency 1 cycle, MSHR queue size 4
L2 (SRAM)	Private, 256KB, 64B cache line, 8-way set-associative, parallel-access, tag latency 1 cycle, data latency 2 cycles, MSHR queue size 8
L3 (STT-MRAM)	shared, 8MB, SRAM tag and STT-MRAM data arrays, 64B cache line, 16-way set-associative, sequential-access, non-inclusive, tag latency 2 cycles, data read latency 9 cycles, data write latency 25 cycles, MSHR and response queue size 64
Main Memory (DRAM)	DDR3, 1600MHz, 8GB, single channel, 2 ranks/channel, 8 banks/rank, page size 1KB.

TABLE II
SPEC WORKLOAD CATEGORIZATION

Category	Benchmarks
L3 Agnostic (LA)	povray, sphinx3, namd, sjeng, astar, gobmk, wrf, bzip2, dealII, gromacs, hmmer, GemsFDTD
L3 Heavy (LH)	gamess, soplex, omnetpp
Memory Heavy (MH)	milc, zeusmp, bwaves, libquantum, leslie3d, mcf, lbm

581 benchmarks (Table II), we execute them in a standalone
 582 environment. While LA applications send fewer accesses to
 583 the LLC, LH and MH applications have most of their accesses
 584 producing LLC hits and misses, respectively. NOVELLA
 585 estimates cache miss rate from performance counters collected
 586 for cumulative LLC miss and access counts. While this
 587 approach captures the long-term behavior of LLC miss rates,
 588 NOVELLA’s reuse-aware careful bypass decisions disturb
 589 LLC reuse minimally, preserving the sanctity of the classifica-
 590 tion (e.g., preventing LH workloads from being misclassified
 591 as MH). Baselines WCAB [3], SHiP [10], OBM [11],
 592 BFP [15], COBRRA [6] and NBB are already discussed in
 593 Sections II and III. We use two different sets of workloads:
 594 1) *sensitivity* and 2) *evaluation*. The sensitivity set consists
 595 of 32 workloads [26] for determining the values of policy
 596 parameters (Section VI-F). Once parameters are finalized, a

597 set of 12 evaluation workloads (Table III) is used for the
 598 final evaluation. Both sets are diverse in their compositions,
 599 created randomly, with more representatives from LH and
 600 MH applications, which are more interesting to us than LA
 601 applications that have limited interactions with LLC. We select
 602 a different set for determining parameters to demonstrate that
 603 parameters tuned on any similar set can effectively work on
 604 the evaluation set.

B. Overall DRAM Energy

605
 606 Fig. 5 illustrates the comparison of total DRAM energy con-
 607 sumption of NOVELLA against six baseline policies across 12
 608 evaluation workloads. The Y-axis shows normalized DRAM
 609 energy, calculated by dividing each policy’s DRAM energy
 610 by that of naïve NBB, with the X-axis showing different
 611 workloads. As shown in Fig. 5, while WCAB [3], SHiP [10],
 612 OBM [11], BFP [15], and COBRRA [6] reduce the overall
 613 DRAM energy consumption by 4%, 4%, 6%, 8%, and 12%,
 614 respectively, over NBB, NOVELLA, with a significant energy
 615 gain of 21%, outperforms all baselines. While WCAB, SHiP,
 616 OBM, and BFP overlook LLC contention, emphasizing LLC
 617 reuse, COBRRA, designed for an SRAM LLC, does not
 618 address all sources of NVM writes and focuses specifically on
 619 system throughput, leading to suboptimal energy gains.

620 For workloads entirely consisting of LH applications (mixes
 621 2 and 3), bypassing writebacks is more energy-efficient. The
 622 AWB policy, discussed in Section III, offers a 28% energy gain
 623 for these mixes, while ARB increases DRAM energy by 25%.
 624 As shown in Fig. 5, WCAB achieves an average energy gain of
 625 14% over NBB. For these LH workloads, BFP and OBM yield
 626 energy gains of 8% and 1%, respectively, while SHiP increases
 627 the DRAM energy by 7%. Although COBRRA exploits the
 628 tradeoff between LLC contention and reuse, it increases
 629 DRAM energy by 5% because it aggressively bypasses
 630 responses and caches writebacks. Nevertheless, NOVELLA,
 631 with adaptive bypass decisions for the two sources of NVM
 632 writes, i.e., writebacks and responses, achieves an energy
 633 saving of 28% across these workloads, outperforming state-
 634 of-the-art techniques by significant margins.

635 Across workloads consisting entirely of MH applications
 636 (mixes 4 and 5), aggressive bypassing (especially of write-
 637 backs) is energy-inefficient. While aggressively bypassing

TABLE III
EVALUATION WORKLOADS

Mix No.	Core 1	Core 2	Core 3	Core 4	Core 5	Core 6	Core 7	Core 8
mix1	wrf	astar	deallI	namd	gromacs	deallI	deallI	sphinx3
mix2	omnetpp	gamsess	omnetpp	gamsess	omnetpp	soplex	gamsess	gamsess
mix3	omnetpp	omnetpp	omnetpp	soplex	omnetpp	omnetpp	omnetpp	gamsess
mix4	libquantum	mcf	lbm	zeusmp	bwaves	libquantum	leslie3d	bwaves
mix5	leslie3d	mcf	libquantum	bwaves	milc	zeusmp	lbm	bwaves
mix6	deallI	gobmk	astar	astar	deallI	bzip2	gamsess	gamsess
mix7	hmmer	bwaves	mcf	leslie3d	lbm	zeusmp	leslie3d	leslie3d
mix8	gamsess	zeusmp	milc	leslie3d	libquantum	mcf	libquantum	zeusmp
mix9	gamsess	gamsess	omnetpp	lbm	bwaves	libquantum	mcf	zeusmp
mix10	soplex	gamsess	omnetpp	gamsess	lbm	zeusmp	zeusmp	mcf
mix11	gamsess	omnetpp	omnetpp	soplex	soplex	soplex	bwaves	leslie3d
mix12	mcf	zeusmp	wrf	sjeng	hmmer	omnetpp	omnetpp	soplex

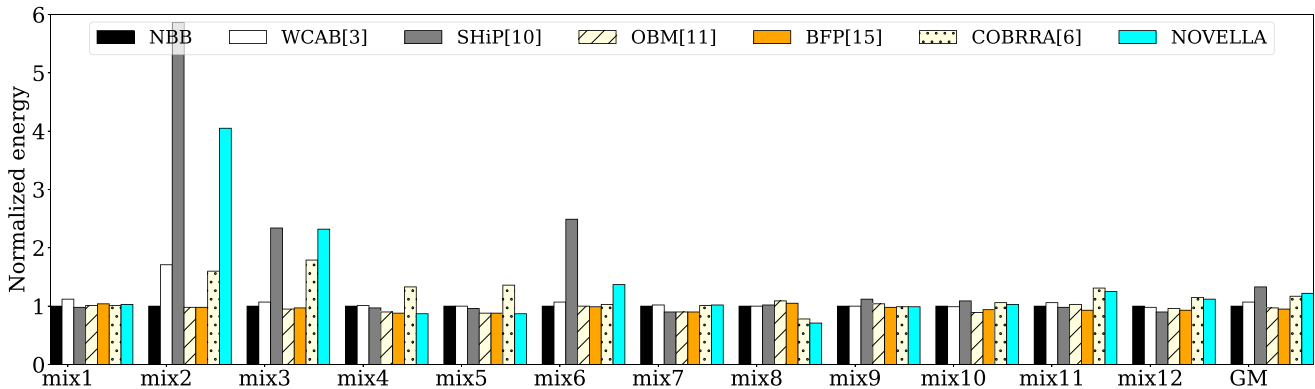


Fig. 6. Comparison of DRAM dynamic energy consumption for NOVELLA and other baselines.

writebacks is found to increase DRAM energy by 8% (AWB of Section III), WCAB, with conservative writeback bypass, shows marginal energy gain. While reuse-emphasizing bypass policies, such as SHiP, OBM, and BFP offer energy gains of 8%, 12%, and 13%, respectively, over NBB, COBRRA increases DRAM energy by 1%, reinforcing the inefficiency of aggressive bypass decisions for these workloads where DRAM is already burdened with LLC misses. However, NOVELLA achieves a 13% reduction in DRAM energy consumption.

For mixes 8-11 co-executing LH and MH applications, NOVELLA offers 27%, 24%, 26%, 25%, and 3% higher-energy gain over baselines WCAB, SHiP, OBM, BFP, and COBRRA, respectively. Selective caching of responses proves energy-efficient for these workloads. For mix1 (LA workload), while WCAB increases DRAM energy by 1%, SHiP, OBM, BFP, COBRRA, and NOVELLA produce energy reductions worth 5%, 1%, 10%, 4%, and 3%, respectively, over NBB.

NOVELLA achieves 9% and 14% higher-energy reductions over bypass strategies using only RPT and only DP, respectively. DP captures a long-term history of response fills, making it suitable for careful bypassing of responses in cases A and B, while the short-term history of fills captured by RPT facilitates the preferred ARB for cases C and D. In cases A and B, the RPT-based reuse criterion tends to bypass responses in an overly aggressive way (82.7% on average), leading to overall energy inefficiency, particularly due to significantly high-DRAM dynamic energy (up to an $8.42\times$ increase over NBB), whereas the DP-based criterion follows a more balanced bypass approach, which is preferred in such

scenarios. Conversely, for cases C and D, the DP-based overly conservative bypass (1.44% of responses) is significantly less efficient than NOVELLA's RPT-based bypass approach, which benefits such workloads by bypassing 67% of responses. This is why we use RPT in cases C and D and DP in cases A and B to determine dead response fills.

We evaluated NOVELLA's energy gains across 5-, 6-, 7-, 9-, and 10-core workloads (apart from 8-core workloads), and observed DRAM energy reductions of 8%, 13%, 16%, 21%, 21%, and 19% compared to NBB across 5-, 6-, 7-, 8-, 9-, and 10-core workloads, respectively.

C. DRAM Energy Breakdown

Figs. 6 and 7 show normalized consumption of different DRAM energy components for the policies across evaluation workloads. Fig. 6 shows that WCAB, SHiP, COBRRA, and NOVELLA increase DRAM dynamic energy by 7%, 33%, 17%, and 22%, respectively, while OBM and BFP reduce it by 3% and 5%. Fig. 7 exhibits that WCAB, SHiP, OBM, BFP, COBRRA, and NOVELLA reduce DRAM static and refresh energies by 5%, 9%, 9%, 9%, 27%, and 32%, respectively, compared to NBB.

Despite increasing DRAM dynamic energy by 35% for LH workloads (mixes 2 and 3), WCAB achieves a 14% overall energy gain by reducing the other energy components by 16%. SHiP increases DRAM dynamic energy by $3.7\times$ compared to NBB, while only marginally reducing other energy components, increasing DRAM energy by 7%. For

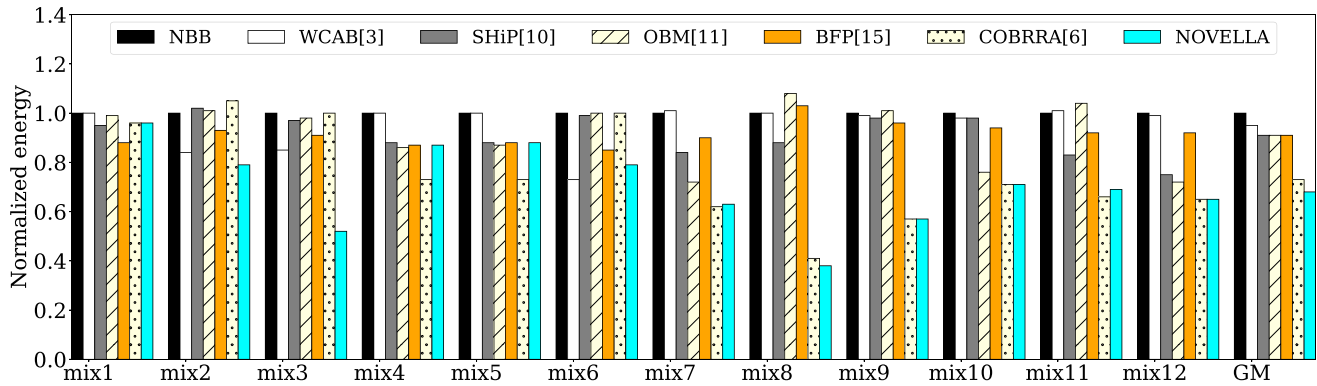


Fig. 7. Comparison of DRAM static and refresh energy consumption for NOVELLA and other baselines.

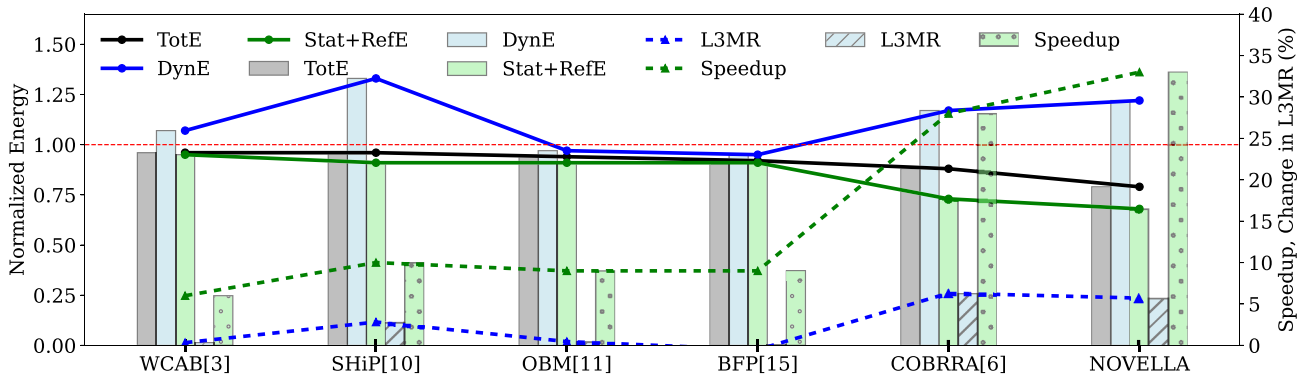


Fig. 8. Summary of key tradeoffs. The LLC miss rate trends align with the DRAM dynamic energy (blue lines), while the performance speedup strongly influences static and refresh energies together (green lines).

694 these mixes, OBM and BFP reduce DRAM’s dynamic energy
 695 by 4% and 3%, and combined static and refresh energies
 696 by 1% and 8%, respectively, over NBB. For these mixes,
 697 responses contribute significantly to LLC reuse. COBRRA’s
 698 ARB increases dynamic energy by 69%, but fails to reduce
 699 static and refresh energies sufficiently, resulting in a 5%
 700 increase in total DRAM energy over NBB. NOVELLA’s
 701 adaptive strategy of bypassing writebacks aggressively and
 702 responses carefully increases dynamic energy by $3.07\times$ over
 703 NBB, but reduce the other energy components by 36%,
 704 resulting in a 28% overall energy gain across these workloads.

705 For workloads consisting solely of MH applications (mixes
 706 4 and 5), While WCAB minimally impacts different energy
 707 components, SHiP improves both dynamic and combined
 708 static and refresh energies by 4% and 12%, respectively, over
 709 NBB, showing an overall energy savings of 8%. OBM and
 710 BFP reduce dynamic energy by 11% and 12% and static and
 711 refresh energies by 14% and 13%, achieving overall energy
 712 gains of 12% and 13%, respectively, over NBB. COBRRA’s
 713 ARB increases DRAM dynamic energy by 34%, and, despite
 714 a 27% reduction in static and refresh energy components,
 715 the overall DRAM energy still increases by 1% compared
 716 to NBB. Because of high-DRAM traffic volume, aggressive
 717 bypass decisions prove energy inefficient. Surpassing all these
 718 energy gains, as shown in Figs. 6 and 7, NOVELLA reduces
 719 both DRAM energy components by 13%, emphasizing the

720 efficiency of dead-probability based conservative response
 721 bypass for these workloads.

722 For mixes 8-11, co-executing LH and MH applications,
 723 while WCAB shows marginal effects (within $\pm 1\%$) on differ-
 724 ent energy components, SHiP increases DRAM dynamic
 725 energy by 5% but achieves a 4% overall energy saving with
 726 an 8% reduction in static and refresh energies. OBM and BFP,
 727 with minimal impact on dynamic energy and 4% reductions
 728 in combined static and refresh energies, offer overall energy
 729 gains of 2% and 3%, respectively. Caching responses very
 730 selectively proves energy efficient for these mixes. While
 731 COBRRA increases dynamic energy by 2% and reduces
 732 other energies by 42%, with an overall energy gain of 25%,
 733 NOVELLA, with its RPT-based bypassing of dead response
 734 fills, improves dynamic and static energy components by 2%
 735 and 43%, respectively, achieving an overall energy gain of
 736 27% over NBB.

D. Summary of Key Trade-Offs

737 Fig. 8 summarizes the key tradeoff between reuse-
 738 dependent (dynamic energy) and performance-dependent
 739 components (static and refresh energies) of DRAM energy.
 740 While the left Y-axis shows normalized consumption of
 741 various DRAM energy components, the right Y-axis displays
 742 percentage improvements in execution time and percentage
 743

744 increases in NVM LLC miss rate. Different baseline policies
 745 are represented along the X-axis, with naive NBB serving as
 746 the global baseline. WCAB, SHiP, OBM, BFP, COBRRA, and
 747 NOVELLA result in normalized static and refresh energies
 748 (combined) of 0.95, 0.91, 0.91, 0.91, 0.73, and 0.68, respec-
 749 tively (solid green trend line, Fig. 8). This strongly correlates
 750 with the performance speedups of 6%, 10%, 9%, 9%, 28%,
 751 and 33%, respectively (dotted green trend line, Fig. 8). The
 752 correlation is high, because of these energy components being
 753 almost proportional to the overall execution time. NOVELLA
 754 reduces average access delays at DRAM, LLC, L2, and L1
 755 caches by 13%, 55%, 43%, and 43%, respectively, compared
 756 to NBB. Since accesses are served in parallel at different
 757 memory levels, these delays are inherently parallel. WCAB,
 758 SHiP, OBM, BFP, COBRRA, and NOVELLA result in nor-
 759 malized DRAM dynamic energy of 1.07, 1.33, 0.97, 0.95,
 760 1.17, 1.22 (solid blue trend line in Fig. 8), correlating with
 761 the trend observed in increases in LLC miss rate of 0.33%,
 762 2.82%, 0.46%, -0.52%, 6.31%, and 5.71% by WCAB, SHiP,
 763 OBM, BFP, COBRRA, and NOVELLA, respectively, over
 764 NBB (dotted blue line in Fig. 8).

765 The trend in overall DRAM energy is determined by the
 766 trends within its energy components. Therefore, in Fig. 8,
 767 the solid black line lies in between the solid blue and
 768 green lines. Because the combined static and refresh energy
 769 is more dominant than the dynamic energy, the overall
 770 energy trend aligns more closely with the trend in these two
 771 components. However, performance efficiency alone is not
 772 sufficient for achieving energy efficiency. Our comprehensive
 773 experimental analysis demonstrates that neither reuse-aware
 774 prior bypass policies, such as WCAB, SHiP, OBM, and BFP,
 775 nor contention- and reuse-aware policies, such as COBRRA,
 776 are the most energy-efficient, underscoring the effectiveness
 777 of NOVELLA.

778 E. LLC and Memory-System Energy

779 Across our workloads, DRAM, LLC, L2, and L1 caches
 780 consume 63.59%, 8.48%, 4.92%, and 23.01% of the whole
 781 memory-system energy, respectively. NOVELLA consistently
 782 reduces the static energy components of DRAM and all
 783 levels of caches by mitigating NVM LLC contention and
 784 improving execution time. Performance improvement reduces
 785 LLC leakage energy by 33%, and bypassing of expensive
 786 NVM writes reduces LLC dynamic energy by 41% compared
 787 to NBB, resulting in an overall LLC energy reduction of 34%
 788 over NBB. While NOVELLA reduces energy consumption of
 789 whole memory hierarchy by 20% over NBB, our optimizations
 790 are independent of processor energy consumption, and there-
 791 fore, can be applied together with core energy optimization
 792 techniques for a system-wide energy efficiency.

793 F. Parameter Selection

794 Parameters of NOVELLA are determined through experi-
 795 ments across 32 sensitivity workloads, discussed as follows:

796 1) *Miss Rate Thresholds*: MR_{ThL} is varied in $\{0, 0.05, 0.1,$
 797 $0.2, 0.3, 0.4, 0.5\}$, resulting in energy gains of 8.6%, 11.2%,
 798 11.6%, 8.8%, 8.9%, 7.9%, and 2.4%, respectively. Higher

799 values, such as 0.8 and 1.0, increase the memory energy by
 800 2.4% and 6.1%, respectively, due to AWB. Therefore, we set
 801 $MR_{ThL} = 0.1$ which leads to the highest-energy reduction.
 802 MR_{ThH} is varied in the range 0.3-1 with a gap of 0.05 in
 803 between, resulting in the energy gain to vary within 5%–12%.
 804 We select $MR_{ThH} = 0.8$ as it produces the highest-energy
 805 gain.

806 2) *Dead Probability Threshold*: We observe the energy
 807 gain to be 10.1%, 9.5%, 11.6%, 11.3%, 11.2%, and 9.2%,
 808 respectively, for DP_{Th} 's value of 0.1, 0.2, 0.3, 0.4, 0.5, and
 809 0.6. We opt for $DP_{Th} = 0.3$ as it leads to the maximum energy
 810 gain.

811 3) *Reuse Predictor Table Size*: We experiment with the
 812 signature width (K) being 7, 8, 9, 10, 11, 12, 13, and 14 LSBs
 813 of the instruction PC. RPTs of 128, 256, 512, 1024, 2048,
 814 4096, 8192, and 16384 entries result in energy gain of 5%, 5%,
 815 6%, 6%, 4%, 12%, 13%, and 12%, respectively. We choose
 816 RPT's size to be 4096 in order to reduce hardware overhead,
 817 without significantly sacrificing energy gain.

818 G. Overhead

819 NOVELLA's decisions do not lie on the critical path because
 820 they are evaluated in parallel with the service of accesses
 821 from LLC controller queues. NOVELLA's energy and area
 822 overheads are estimated using Synopsys technology library,
 823 CACTI, and NVSim for 22nm technology. 9-bit fill and 6-
 824 bit dead counters are added to each LLC line as additional
 825 metadata, increasing tag array size from 720 KB to 960 KB.
 826 NOVELLA's storage (flip-flops, RPT) and logic units incur an
 827 area overhead of 0.0792 mm², which is 3% of total LLC area
 828 (2.64 mm²). Across our workloads, DRAM consumes 0.297
 829 J of energy, with NOVELLA adding an overhead of 0.0035 J,
 830 which is 1.18% of the total DRAM energy.

831 VII. CONCLUSION

832 Addressing energy bottlenecks related to off-chip memory
 833 accesses is crucial for sustainable computing. NOVELLA
 834 reduces off-chip memory energy by exploiting tradeoffs
 835 between LLC contention and reuse through NVM write
 836 bypass. Across SPEC workloads, NOVELLA achieves 21%
 837 and 10.23% higher-energy-savings compared to a no-bypass
 838 solution and a state-of-the-art bypass solution, respectively.
 839 We show that performance-optimal aggressive bypass policies
 840 are not energy-optimal. In the future, we plan to investigate
 841 a coordinated approach for energy-efficiency, involving both
 842 LLC and DRAM controllers. We also plan to study the
 843 problem in the presence of both demand and prefetch traffic.

844 REFERENCES

- 845 [1] A. Boroumand et al., "Google workloads for consumer devices:
 846 Mitigating data movement bottlenecks," in *Proc. 23rd Int. Conf. Archit.*
 847 *Support Program. Lang. Oper. Syst.*, 2018, pp. 316–331.
- 848 [2] A. Salahvarzi, M. Khosroanjani, A. M. H. Monazzah, H. Beitollahi,
 849 U. Y. Ogras, and M. Fazeli, "WiSE: When learning assists resolv-
 850 ing STT-MRAM efficiency challenges," *IEEE Trans. Emerg. Topics*
 851 *Comput.*, vol. 11, no. 1, pp. 43–55, Jan.–Mar. 2023.
- 852 [3] K. Korgaonkar et al., "Density tradeoffs of non-volatile memory as a
 853 replacement for SRAM based last level cache," in *Proc. ACM/IEEE 45th*
 854 *Annu. Int. Symp. Comput. Archit. (ISCA)*, 2018, pp. 315–327.

- 855 [4] S. Tiwari, S. Tuli, I. Ahmad, A. Agarwal, P. R. Panda, and
856 S. Subramoney, "REAL: REquest arbitration in last level caches," *ACM*
857 *Trans. Embedded Comput. Syst.*, vol. 18, no. 6, pp. 1–24, 2019.
- 858 [5] G. Modi, A. Bagchi, N. Jindal, A. Mandal, and P. R. Panda,
859 "CABARRE: Request response arbitration for shared cache manage-
860 ment," *ACM Trans. Embedded Comput. Syst.*, vol. 22, no. 5S, pp. 1–24,
861 2023.
- 862 [6] A. Bagchi, D. Joshi, and P. R. Panda, "COBRRA: Contention-aware
863 cache bypass with request-response arbitration," *ACM Trans. Embedded*
864 *Comput. Syst.*, vol. 23, no. 1, pp. 1–30, 2024.
- 865 [7] J. Ahn, S. Yoo, and K. Choi, "DASCA: Dead write prediction assisted
866 STT-RAM cache architecture," in *Proc. IEEE 20th Int. Symp. High*
867 *Perform. Comput. Archit. (HPCA)*, 2014, pp. 25–36.
- 868 [8] J. Wang, X. Dong, and Y. Xie, "OAP: An obstruction-aware cache
869 management policy for STT-RAM last-level caches," in *Proc. Design,*
870 *Autom. Test Europe Conf. Exhibit. (DATE)*, 2013, pp. 847–852.
- 871 [9] C. Zhang, G. Sun, P. Li, T. Wang, D. Niu, and Y. Chen, "SBAC: A
872 statistics based cache bypassing method for asymmetric-access caches,"
873 in *Proc. Int. Symp. Low Power Electron. Design*, 2014, pp. 345–350.
- 874 [10] C.-J. Wu, A. Jaleel, W. Hasenplaugh, M. Martonosi, S. C. Steely Jr.,
875 and J. Emer, "SHiP: Signature-based hit predictor for high performance
876 caching," in *Proc. 44th Annu. IEEE/ACM Int. Symp. Microarchitecture*,
877 2011, pp. 430–441.
- 878 [11] L. Li, D. Tong, Z. Xie, J. Lu, and X. Cheng, "Optimal bypass monitor
879 for high performance last-level caches," in *Proc. 21st Int. Conf. Parallel*
880 *Archit. Compilation Techn.*, 2012, pp. 315–324.
- 881 [12] K. Kuan and T. Adegbija, "HALLS: An energy-efficient highly adaptable
882 last level STT-RAM cache for multicore systems," *IEEE Trans. Comput.*,
883 vol. 68, no. 11, pp. 1623–1634, Nov. 2019.
- 884 [13] J. Ahn, S. Yoo, and K. Choi, "Write intensity prediction for energy-
885 efficient non-volatile caches," in *Proc. Int. Symp. Low Power Electron.*
886 *Design (ISLPED)*, 2013, pp. 223–228.
- 887 [14] H.-Y. Cheng et al., "LAP: Loop-block aware inclusion properties for
888 energy-efficient asymmetric last level caches," *ACM SIGARCH Comput.*
889 *Archit. News*, vol. 44, no. 3, pp. 103–114, 2016.
- 890 [15] J. J. K. Park, Y. Park, and S. Mahlke, "A bypass first policy for energy-
891 efficient last level caches," in *Proc. Int. Conf. Embedded Comput. Syst.*
892 *Archit. Model. Simulat. (SAMOS)*, 2016, pp. 63–70.
- [16] Z. Wang, D. A. Jiménez, C. Xu, G. Sun, and Y. Xie, "Adaptive placement
893 and migration policy for an STT-RAM-based hybrid cache," in *Proc.*
894 *IEEE 20th Int. Symp. High Perform. Comput. Archit. (HPCA)*, 2014,
895 pp. 13–24.
- [17] K. Kuan and T. Adegbija, "LARS: Logically adaptable retention time
897 STT-RAM cache for embedded systems," in *Proc. Design, Autom. Test*
898 *Europe Conf. Exhibit. (DATE)*, 2018, pp. 461–466.
- [18] M. Baranwal, U. Chugh, S. Dalal, S. Agarwal, and H. K. Kapoor,
900 "DAMUS: Dynamic allocation based on write frequency in multi-
901 retention STT-RAM based last level caches," in *Proc. 22nd Int. Symp.*
902 *Qual. Electron. Design (ISQED)*, 2021, pp. 469–475.
- [19] P. Zhou, B. Zhao, J. Yang, and Y. Zhang, "Energy reduction for STT-
904 RAM using early write termination," in *Proc. Int. Conf. Comput.-Aided*
905 *Design*, 2009, pp. 264–268.
- [20] J. Jung, Y. Nakata, M. Yoshimoto, and H. Kawaguchi, "Energy-efficient
907 spin-transfer torque RAM cache exploiting additional all-zero-data
908 flags," in *Proc. Int. Symp. Qual. Electron. design (ISQED)*, 2013,
909 pp. 216–222.
- [21] D. Shin, H. Jang, K. Oh, and J. W. Lee, "An energy-efficient dram cache
911 architecture for mobile platforms with PCM-based main memory," *ACM*
912 *Trans. Embedded Comput. Syst.*, vol. 21, no. 1, pp. 1–22, 2022.
- [22] D. Wu, B. He, X. Tang, J. Xu, and M. Guo, "RAMzzz: Rank-aware
914 DRAM power management with dynamic migrations and demotions,"
915 in *Proc. Int. Conf. High Perform. Comput., Netw., Storage Anal.*, 2012,
916 pp. 1–11.
- [23] C.-Y. Lai, G.-Y. Pan, H.-K. Kuo, and J.-Y. Jou, "A read-write aware
918 DRAM scheduling for power reduction in multi-core systems," in
919 *Proc. 19th Asia South Pacific Design Autom. Conf. (ASP-DAC)*, 2014,
920 pp. 604–609.
- [24] K. Chandrasekar et al., "DRAMPower: Open-source DRAM power &
922 energy estimation tool," Nov. 2022. [Online]. Available: <https://github.com/tukl-msd/DRAMPower>
- [25] A. Limaye and T. Adegbija, "A workload characterization of the SPEC
925 CPU2017 benchmark suite," in *Proc. IEEE Int. Symp. Perform. Anal.*
926 *Syst. Softw. (ISPASS)*, 2018, pp. 149–158.
- [26] A. Bagchi, O. Rishabh, and P. R. Panda, "NOVELLA: Non-volatile last-
928 level cache bypass for optimizing off-chip memory energy." Jul. 2024.
929 [Online]. Available: <https://github.com/marg-tools/NOVELLA>
- 930